Theory of the Linear Dichroism in the Extended X-ray Absorption Fine Structure (EXAFS) of Partially Vectorially Ordered Systems*

Jens Dittmer and Holger Dau*

Fachbereich Biologie/Botanik, Philipps-Universität Marburg, Lahnberge, D-35032 Marburg, Germany

Received: February 7, 1998; In Final Form: June 16, 1998

Using linearly polarized X-rays for investigations on noncrystalline samples, information on the orientation of the investigated local structure with respect to a nanostructure (e.g., membranes, proteins, layered compounds, and polymers) or a textured macroscopic structure (e.g., a rough surface) may become accessible in case the considered molecular system is partially ordered. For systems with a preferential orientation of one axis of the molecular coordinate system (**M**, e.g., the membrane normal) with respect to a vector in the macroscopic sample system (**S**, typically the normal to the macroscopic sample surface), an equation is derived which describes the dependence of the EXAFS on (i) $\theta_{\mathbf{E}}$, the angle between the X-ray electric field vector and **S**, (ii) a single order parameter, (iii) $\theta_{\mathbf{R}}$, the angle between the absorber-backscatterer vector and **M**. A data-evaluation method is proposed which involves a joint-fit of EXAFS spectra measured for, at least, two excitation angles, $\theta_{\mathbf{E}}$. Our approach accounts correctly for partial disorder; and it allows an exact single-scattering, curved-wave treatment of the EXAFS originating from an absorber−backscatterer pair of unknown orientation. An approximative and the curved-wave approach for evaluation of EXAFS dichroism data are compared.

I. Introduction

Analysis of the extended X-ray absorption fine structure (EXAFS) is frequently employed for structural investigations on noncrystalline samples in physical, chemical, and material sciences.[1−3] Due to increased brilliance of synchrotron radiation sources and improved detection schemes (fluorescence-detected XAS using energy-resolving multi-element solid-state detectors[4]), XAS spectroscopy has recently gained importance in biophysical chemistry as a technique for investigations on metal centers of metallo-enzymes.[1]

Analysis of EXAFS spectra provides precise mean values for the distance between the nuclei of the absorbing atom and the backscattering atom of the first, second, and higher coordination spheres.[5,1−3] In addition, information on coordination numbers and the distance spread (Debye−Waller factors) within the individual coordination spheres becomes available.[1−3] Occasionally, multiple-scattering contributions to the EXAFS can be exploited to determine binding angles.[6] Typically, however, EXAFS spectroscopy on noncrystalline samples does not provide information on binding angles or on the orientation of the investigated local structure with respect to a nanostructure (e.g., a protein or membrane) or a macroscopic structure (e.g., a surface). In some cases these limitations can be, at least partially, overcome by using a linear dichroism approach.

Linear dichroism spectroscopy involves the use of linearly polarized electromagnetic radiation and, typically, some order (or preferential orientation) of the considered molecular system with respect to a coordinate system fixed in the macroscopic sample. Here, we will treat the particularly often encountered case of noncrystalline samples which are partially ordered with respect to a single sample axis (partial vectorial order); for an example, see Figure 1.

* Corresponding author. FB Biologie/Botanik, Philipps-Universität Marburg, Lahnberge D-35032 Marburg (Lahn), Germany. Phone: 49-6421-282078. FAX:49-6421-281545. E-Mail: dauh@mailer.uni-marburg.de.

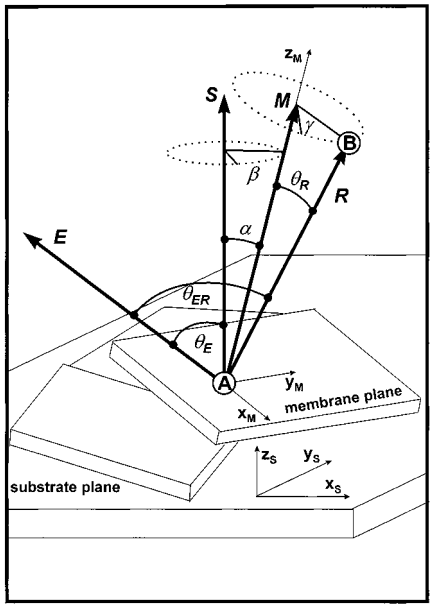

Figure 1. Vectors and angles for partially vectorially-oriented membrane particles. **S**, normal of the macroscopic substrate plane (sample normal) which coincides with the z_S-axis of the sample system; **M**, normal of the membrane plane of the molecular system which coincides with the z_M-axis of the molecular system; **E**, X-ray electric field vector; **R**, the vector connecting the X-ray absorber A and the photoelectron backscatterer B; $\theta_{\mathbf{ER}}$, angle between **E** and **R**; $\theta_{\mathbf{E}}$, angle between **E** and **S**; $\theta_{\mathbf{R}}$, angle between **R** and **M**; α, angle between **M** and **S**. The angles α, β, and γ are the integration variables used in eqs 1 and 6.

In Figure 1, membrane sheets are stacked on some flat substrate such that the preferential orientation of the membrane normal **M** is in parallel to **S**, the normal of the substrate plane (in the following denoted as "sample normal"). The membrane sheet may contain various copies of a metallo-protein (not shown in Figure 1) which carries the absorbing atom A and the

S1089-5647(98)01049-9 CCC: $15.00
Published on Web 08/25/1998

backscattering atom B. A and B are connected by the vector **R**. In all membrane sheets the vector **R** is at the angle $\theta_{\mathbf{R}}$ with respect to the membrane normal **M** (the intrinisc disorder or mosaic spread of **R** with respect to **M** is assumed to be negligible). EXAFS spectra are collected for various angles ($\theta_{\mathbf{E}}$) between the X-ray electric field vector **E** and the sample normal **S**. The EXAFS spectra may depend on $\theta_{\mathbf{E}}$, the excitation angle; this EXAFS dichroism carries structural information which is not accessible by EXAFS spectroscopy on fully disordered (isotropic) samples. It is the main objective of this contribution to derive an exact relation for the $\theta_{\mathbf{E}}$-dependence of spectra of such partially ordered systems (eqs 7 and 8) and to outline applications.

The $\theta_{\mathbf{E}}$-dependence of EXAFS spectra of partially ordered membrane particles has been evaluated quantitatively.[7−11] Here, progress is obtained by treating the disorder influence correctly and by including curved-wave contributions. It should be noted, however, that multiple-scattering effects are not included in the presented theory. Consequently, application of the eventually proposed data-evaluation approach could be problematic in the case of significant interferences of multiple-scattering contributions (which are not unlikely for absorber−backscatterer distances greater than ~3 Å).

The derived dichroism equation for partially vectorially-ordered systems is also of relevance for electronic (dipole) spectroscopy outside the X-ray range. In the present work, however, the main focus is on EXAFS spectroscopy.

Use of the proposed rationale for analysis of the linear dichroism could be advantageous in the case of biological membranes, layered compounds, membrane-free proteins, polymers, and surfaces (see ref 12 and references therein).

II. Results and Discussion

Derivation of the Angle Dependence for a Quantity χ. Two coordinate systems are of relevance: the molecular system which is fixed in the considered individual molecule or molecular structure and the sample system fixed in the macroscopic sample. In the sample system, the *z*-axis is chosen to coincide with a specific unit vector denoted as **S** (e.g., the normal to the substrate plane in Figure 1); the molecular system's *z*-axis is chosen to coincide with a specific unit vector denoted as **M** (e.g., the normal to the surface plane of the membrane sheets in Figure 1). The orientation of the molecular coordinate system with respect to the sample system is described by the Euler angles α, β, and γ (see Figure 1). A distribution function $P(\alpha,\beta,\gamma)$ is defined such that the probability for an orientation of the molecular system which is characterized by the angle triple (α,β,γ) equals $\sin\alpha P(\alpha,\beta,\gamma)$. For fully disordered systems (isotropic case), the distribution function P is independent of α, β, and γ, and $P(\alpha,\beta,\gamma)$ equals $(2\pi)^{-2}$. For a single-crystal sample, P depends on all three Euler angles and is characterized by a distinct number of δ-function-type maxima.

In the following we consider noncrystalline, but partially vectorially ordered system. A system is considered to be partially vectorially ordered if vectors **M** and **S** exist such that $P(\alpha,\beta,\gamma)$ depends solely on α, the angle between **M** and **S**. Thus, for a partially vectorially ordered system:

$$P(\alpha,\beta,\gamma) = P(\alpha)$$

with

$$\int_0^{\pi/2} d\alpha \int_0^{2\pi} d\beta \int_0^{2\pi} d\gamma\, P(\alpha)\sin\alpha = 4\pi^2 \int_0^{\pi/2} P(\alpha)\sin\alpha\, d\alpha = 1 \quad (1)$$

The specific characteristics of the considered system determine $P(\alpha)$. It is often assumed that $P(\alpha)$ is reasonably well approximated by a Gaussian distribution function (i.e., $P(\alpha) \propto \exp(-\alpha^2 \ln 2/\Omega^2)$, where the half-width of the distribution function is given by Ω, the "mosaic spread" angle.[7−11,13,14]

The following derivation is valid for a quantity, χ (e.g., the contribution to the EXAFS spectrum stemming from a single absorber−backscatterer pair of distinct orientation), which is related to the energy ϵ and the direction of the electric field vector of linearly polarized electromagnetic radiation according to

$$\chi(\epsilon,\theta_{\mathbf{ER}}) = \chi^{c}(\epsilon)\cos^2\theta_{\mathbf{ER}} + \chi^{s}(\epsilon)\sin^2\theta_{\mathbf{ER}} \quad (2)$$

In eq 2, $\theta_{\mathbf{ER}}$ is the angle between the electric field vector **E** and a vector, **R**, with a distinct orientation in the molecular coordinate system. (The energy variable ϵ is introduced to stress the relation to spectroscopic experiments.)

The **E**-field unit vector is expressed in Cartesian coordinates of the sample system

$$\mathbf{E}/E = (-\sin\theta_{\mathbf{E}}, 0, \cos\theta_{\mathbf{E}}) \quad (3)$$

where $\theta_{\mathbf{E}}$ is the angle between **E** and the sample normal **S**.

We define the molecular coordinate system such that

$$\mathbf{R}_{\mathrm{M}}/R = (\sin\theta_{\mathbf{R}}, 0, \cos\theta_{\mathbf{R}}) \quad (4)$$

where $\theta_{\mathbf{R}}$ is the angle between **R** and **M**.

Using the Euler matrix $\mathbf{T}_{\mathrm{MS}}$, we obtain for the coordinates of **R**/*R* in the sample system

$$\mathbf{R}_{\mathrm{S}}/R = \mathbf{T}_{\mathrm{MS}}\mathbf{R}_{\mathrm{M}}/R = \begin{pmatrix} (\cos\beta\cos\gamma - \sin\beta\cos\alpha\sin\gamma)\sin\theta_{\mathbf{R}} + \sin\beta\sin\alpha\cos\theta_{\mathbf{R}} \\ (\sin\beta\cos\gamma + \cos\beta\cos\alpha\sin\gamma)\sin\theta_{\mathbf{R}} - \cos\beta\sin\alpha\cos\theta_{\mathbf{R}} \\ \sin\alpha\sin\gamma\sin\theta_{\mathbf{R}} + \cos\alpha\cos\theta_{\mathbf{R}} \end{pmatrix} \quad (5)$$

On basis of eq 2, we obtain in the case of a partially vectorially ordered system for a large ensemble of molecules the integrated, macroscopic χ

$$\chi(\epsilon,\theta_{E}) = \int_0^{\pi/2} d\alpha \int_0^{2\pi} d\beta \int_0^{2\pi} d\gamma\, (\chi^{c}(\epsilon)\cos^2\theta_{\mathbf{ER}} + \chi^{s}(\epsilon)\sin^2\theta_{\mathbf{ER}})P(\alpha)\sin\alpha \quad (6)$$

where $\theta_{\mathbf{ER}}$ is dependent on α, β, γ, $\theta_{\mathbf{E}}$, and $\theta_{\mathbf{R}}$. Using eqs 6 and 1, the equation $\cos^2\theta_{\mathbf{ER}} = (\mathbf{E}/E \cdot \mathbf{R}/R)^2$ and some well-known relations between trigonometric functions, the β- and γ-integration in eq 6 is straightforward. Eventually we obtain

$$\chi(\epsilon,\theta_{\mathbf{E}}) = \frac{1}{3}(\chi^{c} + 2\chi^{s}) + \frac{1}{6}(\chi^{c} - \chi^{s})(3\cos^2\theta_{\mathbf{E}} - 1)(3\cos^2\theta_{\mathbf{R}} - 1)I_{\mathrm{ord}} \quad (7)$$

with

$$I_{\mathrm{ord}} = 2\pi^2 \int_0^{\pi/2} (3\cos^2\alpha - 1)P(\alpha)\sin\alpha\, d\alpha \quad (8)$$

The value of the order integral of eq 8 is zero for an isotropic system and one for a perfectly vectorially ordered system.

Equation 7 is the central result of this contribution. For partially vectorially oriented samples and for quantities which are adequately described by 2, 7 yields the dependence of χ on the macroscopic excitation angle $\theta_{\mathbf{E}}$ in terms of the orientation of **R** in the molecular system ($\theta_{\mathbf{R}}$) and the extent of vectorial order (value of I_{ord}).

For $\theta_{\mathbf{E}} = \arccos\sqrt{1/3} \approx 55°$, the so-called magic angle, the $\theta_{\mathbf{R}}$-dependence of χ vanishes, and $\chi(\epsilon,\theta_{\mathbf{E}}^{\mathbf{magic}})$ is equal to the χ of the corresponding isotropic system. If measurement of a "powder spectrum" is intended, but a fully isotropic **R**-distribution is not guaranteed, measurements at the magic angle are recommendable (see also the magic angle theorem of Pettifer et al.[15]).

Alternative Approaches. George et al. carried out the first EXAFS dichroism investigation on a protein complex, the Photosystem II, embedded in partially ordered membrane sheets as sketched in Figure 1 (for a recent review on Photosystem II-EXAFS, see Yachandra et al.[16]). By means of EPR spectroscopy, they determined the half-width of a Gaussian distribution function which had been used for modeling the disorder in **M**. The evaluation of the EXAFS dichroism by George et al. is based on the erroneous assumption that the orientation of the absorber−backscatter vector **R** (orientation with respect to **S**) is well described by the same Gaussian distribution function (same half-width angle) used for modeling the disorder in **M**. This incorrect (or at least inprecise) approach for evaluation of the EXAFS dichroism also has been used in subsequent investigations.[8−11] For future investigations, we propose to evaluate the EXAFS dichroism of partially vectorially ordered samples on basis of eq 7 (or eq 11) as discussed further below.

Friesner et al. proposed a method which allows calculation of the **E**-distribution function in the molecular system on basis of the **M**-distribution function ($P(\alpha)$ of eq 1).[17,18] This method is, in principle, applicable to the EXAFS dichroism of partially vectorially ordered samples. However, the highly general approach of Friesner et al. involves considerable mathematical intricacies. Using this approach a straightforward, analytical derivation of eq 7 is, in our hands, not possible. (Noteworthily, we found that the approach of Friesner et al. facilitates efficient numerical simulations of EPR spectra of partially ordered samples; Iuzzolino et al., unpublished results.)

Validity Range of Equation 7. The derivation of the dichroism equation, eq 7, is based on eq 2. Due to usage of the dipole approximation and due to the involved rotational symmetry (**R** is the symmetry axis), eq 2 is obtained for the EXAFS originating from a single absorber-backscatterer pair.[19−21] Corresponding equations have been derived for other types of spectroscopic data. In particular, the dependence of the strength of an optical dipole transition on the direction of the **E**-vector is adequately described by eq 2 (**R** corresponds to the transition dipole; $\chi^{\mathrm{s}} = 0$). Consequently, for partially vectorially oriented samples, eq 7 is appropriate for evaluation of optical linear dichroism data. This may be exploited (e.g., for direct experimental determination of the order parameter I_{ord}), in case an optical "probe" with known orientation of its transition dipole (with resepct to **M**) is available.

Today EXAFS experiments are mainly performed at synchrotron radiation sources which deliver radiation characterized by a high degree of polarization. However, dichroism spectroscopy on vectorially ordered samples does not necessarily require polarized x-rays (as pointed out by Brouder[12]). Equation 7 is only valid for linearly polarized light. To derive an equation valid for unpolarized excitation, appropriate averaging of the $\chi(\epsilon,\theta_{\mathbf{E}})$ over the various directions of **E** is required.

EXAFS Dichroism Curved Wave Theory. We apply eq 7 to the contributions of a single absorber−backscatterer pair to the K-edge EXAFS spectrum. In this case, the **R** of eqs 2 and 4 is the distance vector which connects the absorbing and the backscattering atom; the energy dependence of χ is expressed by using an appropriate photoelectron−wavenumber scale (k-scale). A curved-wave treatment of the EXAFS phenomenon results in the following expressions for the χ^{c} and χ^{s} of eq 2:[19−21]

$$\chi^{(\mathrm{c})}(k) = -3\,\mathcal{I}\left(\frac{\mathrm{e}^{2i(kR+\delta_1^{\mathrm{c}})}}{(kR)^2} S_0^2 \mathrm{e}^{-2\sigma^2k^2} \sum_{l=0}^{\infty} (-1)^l t_l \frac{((l+1)c_{l+1} + lc_{l-1})^2}{2l+1}\right) \quad (9)$$

$$\chi^{(\mathrm{s})}(k) = -3\,\mathcal{I}\left(\frac{\mathrm{e}^{2i(kR+\delta_1^{\mathrm{c}})}}{(kR)^2} S_0^2 \mathrm{e}^{-2\sigma^2k^2} \sum_{l=0}^{\infty} (-1)^l t_l {}^1\!/_2 (l+1) \frac{(c_{l+1} - c_{l-1})^2}{2l+1}\right) \quad (10)$$

with

S_0^2, the amplitude reduction factor describing many-particle effects,

$\delta_l^{\mathrm{c}}(k)$, the l=1 phase shift at the central atom

σ, the Debye−Waller parameter

$t_l(k) = \frac{1}{2}(\mathrm{e}^{2i\delta_l} - 1)$, the scattering factors of the partial waves

$c_l(kR) = i^{l+1} kR\, \mathrm{e}^{-ikR} h_l(kR)$, the polynomial part of the spherical Hankel functions h_l

(The superscripts in brackets are used to enable distinction between the specific, theory-dependent functions $\chi^{(\mathrm{c})}$ and $\chi^{(\mathrm{s})}$ of eqs 9 and 10, respectively, and the generalized χ^{c} and χ^{s} of eq 2.)

Insertion into eq 7 yields (using some basic relations between Hankel functions)

$$\chi(k) = -\mathcal{I}\left(\frac{\mathrm{e}^{2i(kR+\delta_1^{\mathrm{c}})}}{(kR)^2} S_0^2 \mathrm{e}^{-2\sigma^2k^2} \sum_{l=0}^{\infty} (-1)^l t_l(k) (g_l^{(\mathrm{iso})} + g_l^{(\mathrm{aniso})} (3\cos^2\theta_{\boldsymbol{E}} - 1)(3\cos^2\theta_{\boldsymbol{R}} - 1) I_{\mathrm{ord}})\right) \quad (11)$$

$$g_l^{(\mathrm{iso})} = (l+1)c_{l+1}^2 + lc_{l-1}^2 \quad (12)$$

$$g_l^{(\mathrm{aniso})} = g_l^{(\mathrm{iso})} - \frac{3}{2} l(l+1) \frac{(c_{l+1} - c_{l-1})^2}{2l+1} \quad (13)$$

The angle-independent, isotropic part of $\chi(k)$ corresponds to the usual EXAFS formula.[19] Figure 2 illustrates the meaning of eq 11−13 for perfect vectorial order (solid lines in Figure 2A) and a partially disordered system (solid lines in Figure 2B). In both cases, the 55°-spectrum corresponds to the spectrum of an isotropic sample. The dichroism (i.e., the extent of the $\theta_{\boldsymbol{E}}$-dependence of the spectra) increases with the degree of order.

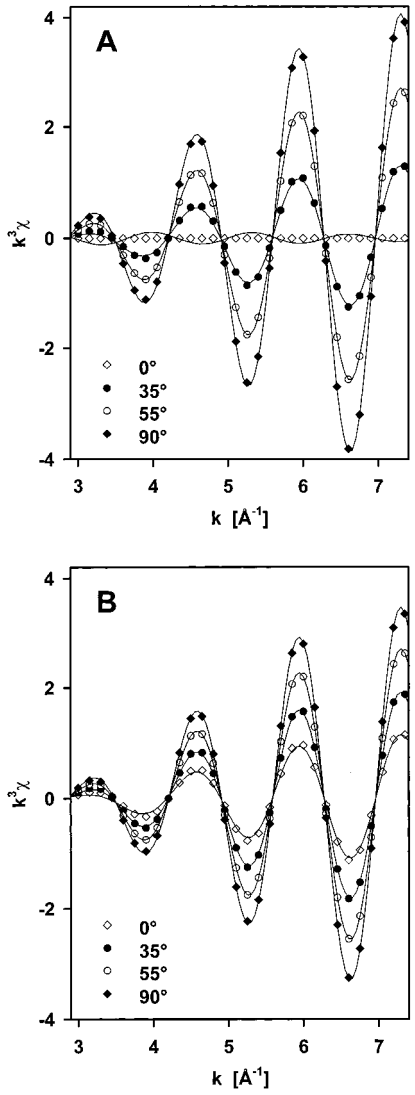

Figure 2. Simulation of k^3-weighted EXAFS spectra for absorption and backscattering by manganese atoms with a nucleus-to-nucleus distance of 2.7 Å. (A) Perfect vectorial order ($I_{ord} = 1$). (B) Gaussian distribution function for P(α) with the half-width angle, $\Omega = 30°$ ($I_{ord} = 0.56$). Solid lines: exact calculation (eq 11-13). Symbols: approximation (eqs 18-20). For calculation of $\chi^{(c)}$ and $\chi^{(s)}$ the program FEFF 6.01[19,23] (using $S_0 = 1$, $\sigma^2 = 0.0025$ Å^2) has been employed .

Remarkably in Figure 2A, the sign of the EXAFS functions changes when θ_E approaches 0°.

Multiple Backscatterers per Coordination Shell. Frequently, a coordination shell of the absorbing atom consists of several backscattering atoms of the same type and at the same distance. Assuming N backscattering atoms, we obtain

$$\chi(k,\theta_{\mathbf{E}}) = \frac{1}{3}N\Big((\chi^{c}(k) + 2\chi^{s}(k)) + \frac{1}{2}(\chi^{c}(k) - \chi^{s}(k))(3\cos^2\theta_{\mathbf{E}} - 1)(3\cos^2\bar{\theta}_{\mathbf{R}} - 1)I_{ord}\Big) \quad (14)$$

where $\bar{\theta}_R$, the average angle, is defined by the relation

$$\cos^2\bar{\theta}_R = \frac{1}{N}\sum_{i=1}^{N}\cos^2\theta_{\mathbf{R}_i} \quad (15)$$

For example, for an undistorted octahedral or a tetrahedral coordination sphere, $\bar{\theta}_{\mathbf{R}}$ is equal to the magic angle; no EXAFS dichroism is predicted. For square-planar coordination, $\bar{\theta}_{\mathbf{R}}$ is restricted to values ranging from 45° to 90°.

Curved-Wave Joint-Fit Approach for Data Evaluation. Rewriting eq 14 yields

$$\chi(k,\theta_{\mathbf{E}}) = N(\chi^{iso}(k,R,\sigma) + \chi^{aniso}(k,R,\sigma)(3\cos^2\theta_{\mathbf{E}} - 1)A) \quad (16)$$

with

$$A = (3\cos^2\bar{\theta}_R - 1)I_{ord} \quad (17)$$

Typically, the data evaluation will aim at the determination of R, σ, N, and of $\bar{\theta}_{\mathbf{R}}$ by using an appropriate curve-fit approach. It is immediately apparent that the determination of $\bar{\theta}_{\mathbf{R}}$ requires determination of I_{ord} by an independent method. Because the k-dependence of χ^{iso} and χ^{aniso} is similar, determination of N and A (and thus $\bar{\theta}_{\mathbf{R}}$) requires that EXAFS spectra for at least two different $\theta_{\mathbf{E}}$ are available. Noteworthily, data collected at any two excitation angles contain the full information accessible by EXAFS dichroism measurement. However, due to the usually inevitable noise, it is advisable to collect spectra at various angles covering a $\theta_{\mathbf{E}}$-range which is as large as experimentally feasible.

We propose to determine N and A on the basis eq 16 by a simultaneous fit of spectra collected at several distinct angles using the same R-value and the same σ-value for all angles (joint-fit approach). Two advantages are associated with this joint-fit approach: (i) application of the curved-wave theory to EXAFS data obtained for partially oriented data becomes feasible, and (ii) there is a significant reduction in the number of fit parameters (in comparison to separate fits of the individual spectra).

EXAFS Dichroism: An Approximative Approach. Because it is not possible to use a curve-fit approach which is based on eqs 11 and 14 with existing software packages, an approximative two-step approach was employed.[14] In the following, this approach is outlined and the involved approximation is discussed in comparison to the exact treatment.

For EXAFS K-edge spectra, usually χ^s is clearly smaller than χ^c. In the plane-wave theory or in the small atom approximation the χ^s-contribution is neglected.[22] Therefore, we neglect the χ^s-contribution in eq 14 ($\chi^s = 0$), and we obtain

$$\chi(k) = N_{app}\,\chi^{(iso)}(k) \quad (18)$$

with

$$\chi^{(iso)}(k) = \frac{1}{3}\chi^{c}(k) \quad (19)$$

and

$$N_{app} = NF_{AB} = N\Big(1 + \frac{1}{2}(3\cos^2\theta_{\mathbf{E}} - 1)(3\cos^2\bar{\theta}_{\mathbf{R}} - 1)I_{ord}\Big) \quad (20)$$

The two-step data evaluation approach involves (i) performing a standard, curved-wave EXAFS fit for the individual spectra (same model function for all $\theta_{\mathbf{E}}$). This provides an apparent coordination number N_{app} which depends on $\theta_{\mathbf{E}}$. (ii) Determination of $\theta_{\mathbf{R}}$ by simulation of $N_{app}(\theta_{\mathbf{E}})$ on basis of the approximative eq 20.

The data points in Figure 2 (open and closed symbols) stem from calculations on basis of eqs 18−20 for $\chi^{(iso)} = {}^1/_3\chi^c = {}^1/_3(\chi^{(c)} + 2\chi^{(s)})$ with $\chi^{(c)}$ and $\chi^{(s)}$ calculated according to eqs 9

and 10, respectively. We conclude that in a well-ordered system distinct deviations from results obtained by an exact treatment (solid lines in Figure 2) are apparent for $k < 5$ Å^{-1}. In case the difference between $\theta_{\mathbf{E}}$ and $\theta_{\mathbf{R}}$ approaches 90°, the discrepancies seem to be particularly pronounced and no longer negligible.

Approximate versus Exact, Curved-Wave Treatment. For the example shown in Figure 2A (simulations for $I_{ord} = 1$), a fit of the exact, curved-wave χ by the approximate function fails for $\theta_E = 0$ (tendency to obtain negative values for N_{app}); the approximative approach is not applicable.

On a first glance Figure 2B (simulations for $I_{ord} = 0.56$) appears to indicate that in the case of significant disorder the deviations between the exact, curved-wave and the approximate EXAFS functions is negligible. However, by a decrease of I_{ord} the deviations between curved-wave and approximative χ as well as the dichroism in the EXAFS spectra are reduced (to the same extent, see eq 7 or 14); application of the approximative data-evaluation approach to the curved-wave χ is likely to result in retrieval of inaccurate values for $\theta_{\mathbf{R}}$.

In conclusion, the use of the approximative approach could cause an undesired inaccuracy of the $\theta_{\mathbf{R}}$-determination. Often the approximative approach might yield sufficiently accurate results; nonetheless, there is no decisive advantage associated with its usage. Therefore, and because of the already discussed benefits of the joint-fit method, we recommend to use the exact curved-wave joint-fit approach in the future.

Acknowledgment. We thank the German BMBF (Förderprogramm: Erforschung kondensierter Materie, Verbund 48) for financial support. The presented theoretical developments have profited by a NATO collaborative research grant (Yachandra/Dau). H.D. thanks K. Sauer, M. Klein, and V. Yachandra (Berkeley) for the joint investigations in 1992 which stimulated this work. We are grateful to L. Iuzzolino, H. Schiller, and W. Dörner (Marburg) who collected the EXAFS and EPR data used for tests of the proposed EXAFS data evaluation approach; and we thank H.-F. Nolting, A. Solé, and W. Meyer-Klaucke (Hamburg) for their support with respect to the EXAFS data collection.

References and Notes

(1) Eisenberger, P.; Kincaid, B. M. *Science* **1978**, *200*, 1441.
(2) Lee, P. A.; Citrin, P. H.; Eisenberger, P.; Kincaid, B. M. *Rev. Mod. Phys.* **1981**, *53*, 769.
(3) Teo, B. K. *EXAFS: Basic Principles and Data Analysis*; Springer-Verlag: Berlin, 1986; Chapter 2.
(4) Jaclevic, J.; Kirby, J. A.; Klein, M. P.; Robertson, A. S.; Brown, G.; Eisenberger, P. *Solid State Commun.* **1977**, *23*, 679.
(5) Sayers, D. E.; Stern, E. A.; Lytle, F. W. *Phys. Rev. Lett.* **1971**, *27*, 1204.
(6) Binsted, N.; Strange, R. W.; Hasnain, S. S. *Biochemistry* **1992**, *31*, 12117.
(7) George, G. N.; Prince, R. C.; Cramer, S. P. *Science* **1989**, *243*, 789.
(8) Yachandra, V. K.; DeRose, V. J.; Latimer, M. J.; Mukerji, I.; Sauer, K.; Klein, M. P. *Science* **1993**, *260*, 675.
(9) Mukerji, I.; Andrews, J. C.; DeRose, V. J.; Latimer, M. J.; Yachandra, V. K.; Sauer, K.; Klein, M. P. *Biochemistry* **1994**, *33*, 9712.
(10) Dau, H.; Andrews, J. C.; Roelofs, T. A.; Latimer, M. J.; Liang, W.; Yachandra, V. K.; Sauer, K.; Klein, M. P. *Biochemistry* **1995**, *34*, 5274.
(11) George, G. N.; Cramer, S. P.; Frey, T. G.; Prince, R. C. *Biochim. Biophys. Acta* **1993**, *1142*, 240.
(12) Brouder, C. *J. Phys.: Condensed Matter* **1990**, *2*, 701.
(13) Blum, H.; Salerno, J. C.; Leigh, J. S., Jr. *J. Magn. Resonance* **1977**, *30*, 385.
(14) Schiller, H.; Dittmer, J.; Iuzzolino, L.; Dörner, W.; Meyer-Klaucke, W.; Solé, V. A.; Nolting, H.-F.; Dau, H. *Biochemistry* **1998**, *37*, 7340.
(15) Pettifer, R. F.; Brouder, C.; Benfatto, M.; Natoli, C. R.; Hermes, C.; Ruiz López, M. F. *Phys. Rev. B* **1990**, *42*, 37.
(16) Yachandra, V. K.; Sauer, K.; Klein, M. P. *Chem. Rev.* **1996**, *96*, 2927.
(17) Friesner, R.; Nairn, J. A.; Sauer, K. *J. Chem. Phys.* **1979**, *71*, 358.
(18) Friesner, R.; Nairn, J. A.; Sauer, K. *J. Chem. Phys.* **1980**, *72*, 221.
(19) Mustre de Leon, J.; Rehr, J. J.; Zabinsky, S. I.; Albers, R.C. *Phys. Rev. B* **1991**, *44*, 4146.
(20) Benfatto, M.; Natoli, C. R.; Brouder, C.; Pettifer, R. F.; Ruiz López, M. F. *Phys. Rev. B* **1989**, *39*, 1936.
(21) Barton, J. J; Shirley, D. A. *Phys. Rev. B* **1985**, *32*, 1892.
(22) Gurman, S. J. *J. Phys. C* **1988**, *21*, 3699.
(23) Rehr, J. J.; Mustre de Leon, J.; Zabinsky, S. I.; Albers, R. C. *J. Am. Chem. Soc.* **1991**, *113*, 5135.